International Journal of Computational Bioinformatics and In Silico Modeling
Vol. 2, No. 4 (2013): 206-212
Research Article
Open Access

ISSN: 2320-0634

Prediction of the possible inhibitory effect of 6-(methylsulfinyl)hexyl isothiocyanate (6MITC) and its analogs on P-glycoprotein (P-gp) by *in silico* analysis of their interaction energies

Hideaki Yamaguchi[1]*, Katsuyoshi Kamiie[2], Yumi Kidachi[2], Toshiro Noshita[3], Hironori Umetsu[4], Yoko Fuke[5], Kazuo Ryoyama[2]

[1] *Department of Pharmacy, Faculty of Pharmacy, Meijo University, 150 Yagotoyama, Tenpaku, Nagoya 468-8503, Japan*
[2] *Department of Pharmacy, Faculty of Pharmaceutical Sciences, Aomori University, 2-3-1 Kobata, Aomori 030-0943, Japan*
[3] *Department of Life Sciences, Faculty of Life and Environmental Sciences, Prefectural University of Hiroshima, 562 Nanatsuka, Shobara 727-0023, Japan*
[4] *Laboratory of Food Chemistry, Department of Life Sciences, Junior College, Gifu Shotoku Gakuen University, 1-38 Nakauzura, Gifu 055-8288, Japan*
[5] *Department of Health Promotion Sciences, Graduate School of Human Health Sciences, Tokyo Metropolitan University, 1-1 Minamiosawa, Hachioji 192-0397, Japan*

*Corresponding author: Hideaki Yamaguchi; e-mail: hyamagu@meijo-u.ac.jp

Received: 06 July 2013 Accepted: 26 July 2013 Online: 01 August 2013

ABSTRACT

In the present study, we performed *in silico* analyses of the ligand-residue interaction energies between P-glycoprotein (P-gp) and 6-(methylsulfinyl)hexyl isothiocyanate (6MITC) and its analogs to predict possible inhibitory effect of the ITCs on P-gp. In total, 12 residues were identified as the preferred interaction residues in P-gp. Possible involvement of the moieties at C6 of the ITCs in forming hydrogen bonds in the ITC/P-gp complexes was revealed. Five of the eight tested ITCs had hydrogen bonds with either Asn-721 or Gln-725, indicating that these residues may play important roles in the ITC/P-gp interactions. Further, on the basis of the highest values for the ITC/P-gp interaction energies, the possible accumulation of the ITCs in cells was predicted in the order of 6MITC > 2b > 2e > 2c ≈ 2d ≈ 2h ≈ 2f ≈ 2g. To the best of our knowledge, this is the first report to predict possible inhibitory effect of ITCs on P-gp with *in silico* structural analyses of the ligand-receptor interaction between ITCs and P-gp.

Keywords: 6-(Methylsulfinyl)hexyl isothiocyanate (6MITC); ATP-binding cassette (ABC) transpoters; *in silico*; P-glycoprotein (P-gp); structural analysis

ABBREVIATIONS

ABC, ATP-binding cassette; ASE-Dock, alpha sphere and excluded volume-based ligand-protein docking; ITC, isothiocyanate; MDR, multidrug resistance; MOE, Molecular Operating Environment; P-gp, P-glycoprotein; 6MITC, 6-(methylsulfinyl)hexyl isothiocyanate

INTRODUCTION

Isothiocyanates (ITCs) occur widely and abundantly as thioglycoside conjugates known as glucosinolates in *Brassica* species, such as broccoli, brussel sprouts, cabbage, cauliflower, kale, wasabi, and watercress, and *Raphanus* species, such as daikons and radishes [1,2]. Glucosinolates are hydrolyzed by myrosinase (β-thioglucoside glucohydrolase) and ITCs are formed by a Lossen rearrangement [3]. In humans, such reactions can be catalyzed by intestinal microflora [4]. Many standard chemotherapeutic agents, such as cytarabine and daunorubicin, have been found in natural sources,

and since ITCs are present in the above edible plants and consumed by humans in considerable quantities [5,6], they may offer preventive and therapeutic activities against degenerative diseases, such as cancer [7]. In fact, ITCs have been drawing much attention because of findings from *in vitro* and *in vivo* models that they offer possible chemoprotection and chemotherapy against cancer [3, 8, 9]. ITCs have been reported to induce apoptosis in several cancer cell lines, and have been tested in animal models for leukemia, breast cancer, colon cancer, and prostate cancer [10-14]. The factors targeted by ITCs for controlling cancer are antioxidant response elements, Bax, caspases, cyclin A, cyclin B1, cyclin D1, cytochrome P450, Kruppel-like factor 4, p21, p53, and poly ADP-ribose polymerase [15-20]. Modulation of carcinogen metabolism through induction of phase 2 enzymes and/or inhibition of phase 1 enzymes also plays a role in the anticancer activities of ITCs [21-25]. Furthermore, the PI3K/Akt signaling pathway was found to be largely involved in the survival of cancer cells, and an ITC sulforaphane restricted this pathway and inhibited the cell growth [26].

ATP-binding cassette (ABC) transporters are involved in the absorption and elimination of compounds, and act as efflux pumps at cellular membranes to transport molecules against concentration gradients. For some compounds, such as anticancer drugs, that are structurally and/or functionally unrelated to cells, ABC transporters export them across cell membranes and decrease the intracellular concentrations of these foreign compounds [27]. ABC transporters are endogenously expressed in normal cells, but overexpressed in cancer cells. Consequently, they actively export anticancer drugs, decrease the concentrations of the drugs below therapeutic thresholds, and confer multidrug resistance (MDR) on cancer cells. MDR is one of the major problems that needs to be overcome in chemotherapy [28]. P-glycoprotein (P-gp) is an ABC transporter and often overexpressed in MDR cancer cells. It acts as an ATP-dependent efflux pump to transfer a wide variety of compounds, including chemotherapeutic agents. P-gp has also been positively correlated with poor prognosis in cancers. Anthracyclines, epipodophyllotoxins, taxanes, and vinca alkaloids are examples of anticancer drugs that have been identified as substrates of P-gp [29]. P-gp has also been studied for its interactions with ITCs, and certain ITCs showed inhibitory effects on P-gp [30]. Recently, we found that a naturally occurring ITC from wasabi (*Wasabia japonica*), a Japanese indigenous herb, exhibited significant growth inhibitory activity toward a macrophage-like tumor cell line [31]. We have been focusing our attention on the ITC 6-(methylsulfinyl)hexyl isothiocyanate (6MITC) as a possible new candidate for controlling cancer cell progression and metastasis. 6MITC suppressed the growth and survival of breast cancer and melanoma cell lines [32], and also showed anticancer activity in a mouse model of pulmonary metastasis [33]. Taken together, these findings suggest that targeting P-gp with inhibitors from natural origins, such as 6MITC, can be utilized as a potential therapeutic option for controlling cancer.

In the present study, in light of the above-described anticancer activity of 6MITC, we performed ligand fitting of 6MITC and its analogs to P-gp with a molecular modeling method to estimate their possible effects on the P-gp mediated efflux.

MATERIALS AND METHODS

Homology modeling of human P-gp

Homology modeling of human P-gp and its binding site selection and exploration were carried out as previously reported [34]. Briefly, mouse P-gp (PDB code: 3G5U) [35] was selected as a template for the structural modeling of human P-gp (NCBI reference sequence: NP_000918.2) because of its good crystal structure resolution (3.8 Å) and because its information was recent (from 2009) among the reported P-gp models. For construction of the P-gp model, 100 independent models of the target protein were built using a Boltzmann-weighted randomized modeling procedure in Molecular Operating Environment 2011.10 (MOE; Chemical Computing Group Inc., Montreal, Canada) that was adapted from reports by Levitt [36] and Fechteler *et al.* [37]. The intermediate models were evaluated by a residue-packing quality function, which was sensitive to the degrees to which nonpolar side-chain groups were buried and hydrogen-bonding opportunities were satisfied. The P-gp model with the best residue-packing quality function and full energy minimization was selected for further analyses.

In silico ligand-receptor interactions between P-gp and 6MITC and its analogs

Hydrophobic or hydrophilic alpha spheres, which were created by the Site Finder module of the MOE, were utilized to define potential ligand-binding sites (LBSs). Analyses of the ligand-receptor interactions between the ITCs (the structures of 6MITC and its analogs are shown in Figure 1 [31]) and the P-gp model were performed with the alpha sphere and excluded volume-based ligand-protein docking (ASE-Dock) module of the MOE [38]. In the ASE-Dock module, ligand atoms had alpha spheres within 1 Å. Based on this property, concave models were created and ligand atoms from a large number of conformations generated by superimposition with these points were evaluated and scored by the maximum overlap with the alpha spheres and minimum overlap with the receptor atoms. The ligand conformations were subjected to energy minimization using the MMF94S force field [39], and 500 conformations were generated using the default systematic search parameters. Five thousand poses per conformation were randomly placed onto the alpha spheres located within the LBS in P-gp. From the resulting 500,000 poses, 200 poses were selected for further optimization with the MMF94S force field. During the refinement step, the ligands were free to move within the binding pocket.

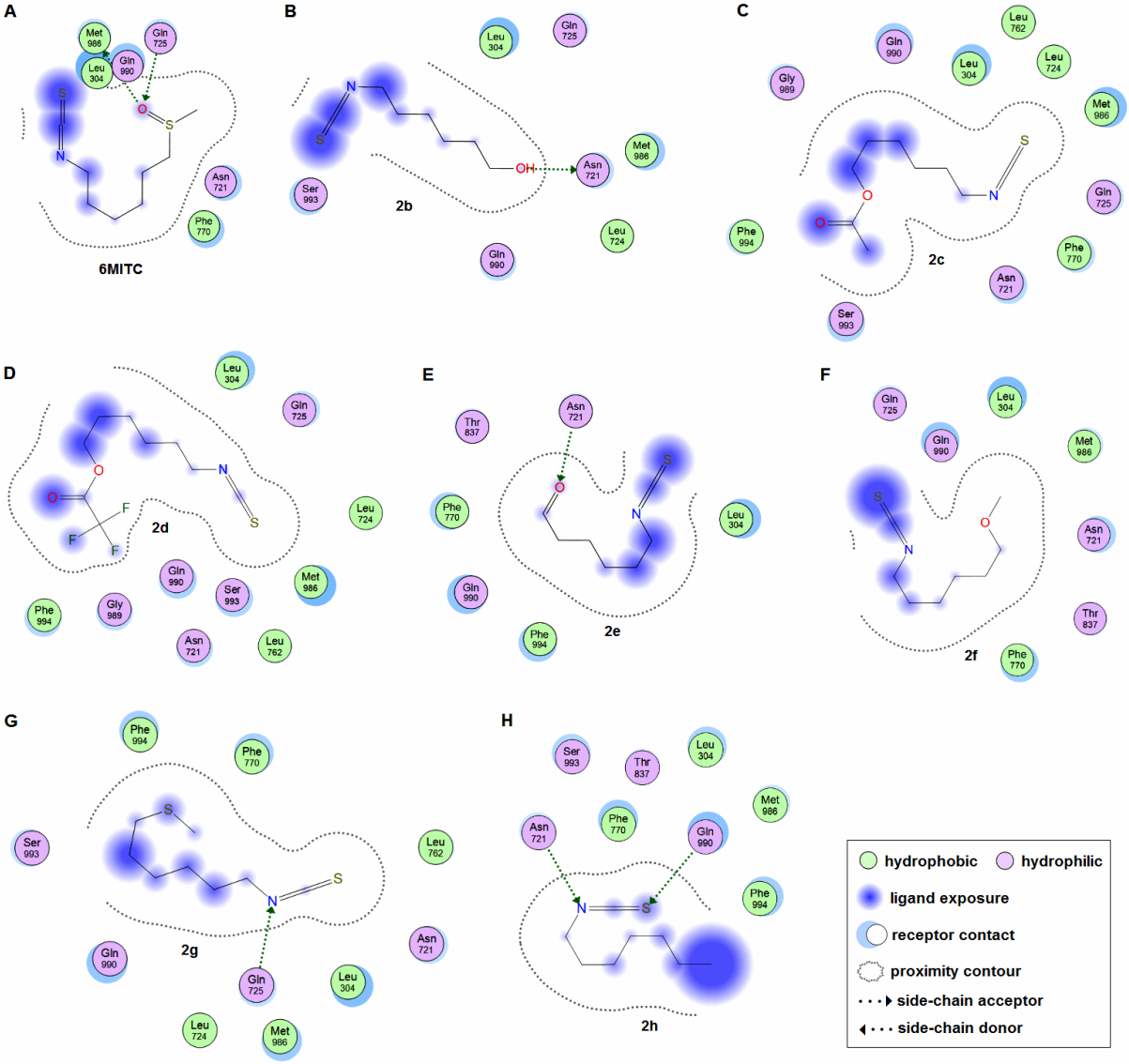

Figure 2. Ligand-receptor interaction plots for the tested ITC/P-gp complexes. (A–H) All of the tested ITCs can bind to the LBS in the P-gp model. (A) The S=O oxygen at C6 of 6MITC is identified as an element that forms hydrogen bonds with Gln-725 and Met-986. (B) The presence of a hydrogen bond is found between the hydroxyl group of 2b at C6 and Asn-721. (C) The 2c/P-gp complex. (D) The 2d/P-gp complex. (E) The C=O oxygen at C6 of 2e forms a hydrogen bond with Asn-721. (F) The 2f/P-gp complex. (G) The presence of a hydrogen bond is found between 2g and Gln-725. (H) The presence of hydrogen bonds is found between 2h and Asn-721 and Gln-990.

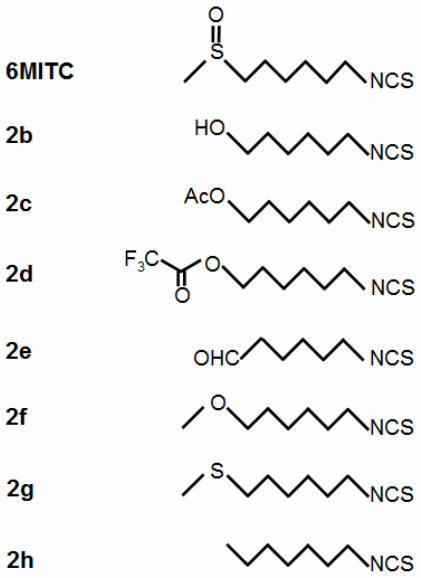

Figure 1. Structures of 6MITC and its analogs used in the present study.

RESULTS AND DISCUSSION

In silico structural analysis of the tested ITC/P-gp models

Although ITCs are prospective naturally-derived anticancer compounds, they are xenobiotics in humans and destined to be exported from or metabolized in cells. ABC transporters, such as P-gp, are involved in the elimination of such foreign compounds and ITCs can be substrates of P-gp [40]. Interestingly, no difference was found between the LBSs of the substrates and inhibitors for P-gp [41], and therefore ITCs have also been reported to be inhibitors of P-gp [30]. In the present study, to predict the inhibitory effects of 6MITC and its analogs on P-gp, we first performed *in silico* structural analyses of the tested ITC/P-gp model to ascertain whether the ITCs could bind to P-gp. Our previous analyses of the structural properties of P-gp and docking simulations of 6MITC/P-gp complexes suggested that our methods

were capable of generating a P-gp model that was similar to the near-native P-gp [34]. To create ligand-receptor interaction plots for each ITC/P-gp complex, the Ligand Interactions module of the MOE was used, which provided a clearer arrangement of the key intermolecular interactions that aid in the interpretation of the 3D juxtaposition of the ligands and the LBS in P-gp. The ASE-Dock module of the MOE [42] revealed that, in addition to 6MITC, all the other tested ITCs could bind to the LBS in the P-gp model (Figure 2A–H). In total, 12 residues were identified as the preferred interaction residues, and the presence of hydrogen bonds was found between 6MITC and Gln-725 and Met-986 (Figure 2A), 2b and Asn-721 (Figure 2B), 2e and Asn-721 (Figure 2E), 2g and Gln-725 (Figure 2G), and 2h and Asn-721 and Gln-990 (Figure 2H). The S=O oxygen at C6 of 6MITC was identified as the element that formed the hydrogen bonds with Gln-725 and Met-986 (Figure 2A). The presence of a hydrogen bond was also found between the hydroxyl group of 2b at C6 and Asn-721 (Figure 2B). Furthermore, the C=O oxygen at C6 of 2e formed a hydrogen bond with Asn-721 (Figure 2E). The isothiocyanato (-NCS; one end of the ITCs) group of ITCs undergoes conjugation with GSH to form dithiocarbamates [43]. Our present results revealed the involvement of the moieties at C6 (other end of the ITCs) of the ITCs in forming hydrogen bonds in the ITC/P-gp complexes. Five of the eight tested ITCs had hydrogen bonds with either Asn-721 or Gln-725 (Figures 2A, B, E, G, and H), indicating that these residues may play important roles in the ITC/P-gp interactions.

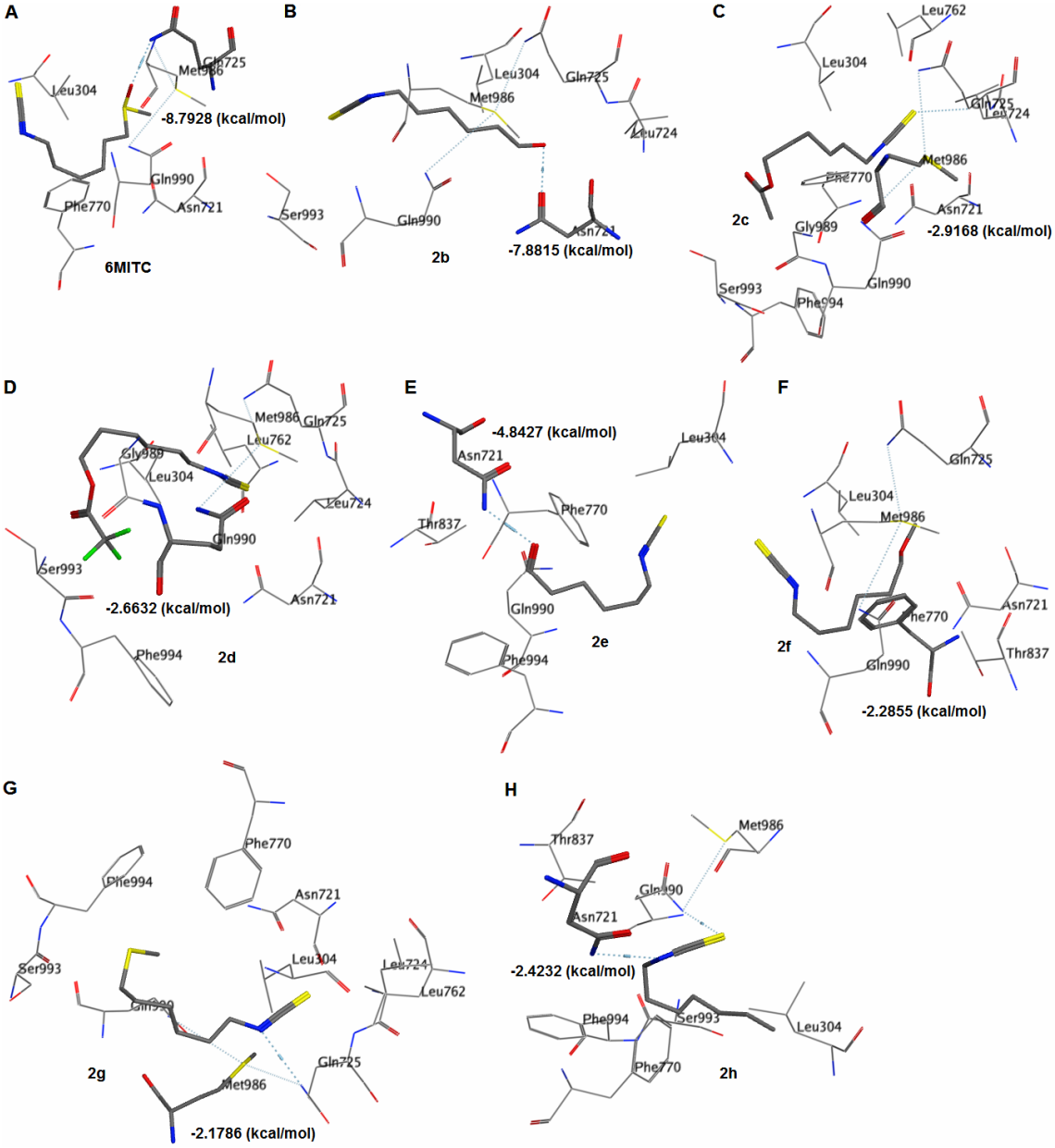

Figure 3. 3D structures of the LBS and the highest interaction energy values for each ITC/P-gp complex. (A) Among the tested structures, 6MITC/Gln-725 has the highest interaction energy value of −8.7928 kcal/mol. (B) 2b/Asn-721 has a value of −7.8815 kcal/mol. (C) 2c/Met-986 has a value of −2.9168 kcal/mol. (D) 2d/Gln-990 has a value of −2.6632 kcal/mol. (E) 2e/Asn-721 has a value of −4.8427 kcal/mol. (F) 2f/Phe-770 has a value of −2.2855 kcal/mol. (G) 2g/Met-986 has a value of −2.1786 kcal/mol. (H) 2h/Asn-721 has a value of −2.4232 kcal/mol. *Blue*: nitrogen; *gray*: carbon; *red*: oxygen; *yellow*: sulfur.

A

Ligand-residue interaction energy (kcal/mol)

	Leu304	Asn721	Leu724	Gln725	Leu762	Phe770	Thr837	Met986	Gly989	Gln990	Ser993	Phe994
6MITC	-1.0132	-3.7562		-8.7928		-0.1927		0.6327		0.2509		
2b	-0.4411	-7.8815	-1.0662	-1.4388				-1.8608		-1.235	-0.1718	
2c	-0.4128	-1.3847	-1.0137	0.0801	-0.2512	-1.5127		-2.9168	-1.2939	-0.8322	-0.5558	-1.6208
2d	-0.064	-0.5301	-0.8168	-1.1624	0.1267			-2.2552	-2.3331	-2.6632	-1.2898	-1.9445
2e	-1.5023	-4.8427				-1.3652	-0.1783			-0.8044		-1.1627
2f	-1.9322	-1.219		-0.2859		-2.2855	-1.2033	-1.7615		-0.2734		
2g	-1.6989	-0.2395	-0.8619	-1.7982	-0.4893	-1.9243		-2.1786		0.1221	-1.1305	-1.645
2h	-0.9972	-2.4232				-0.5371	-0.5961	-0.9911		-0.0065	-1.2251	-1.1832

B

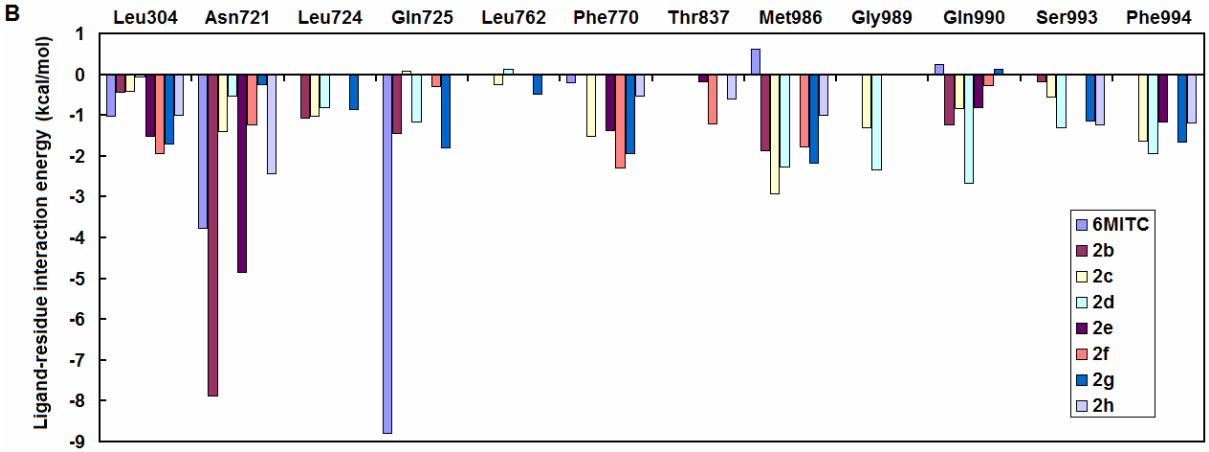

Figure 4. Ligand-residue interaction energies for the 12 preferred residues. (A) The highest values for the 2d, 2f, and 2g/P-gp ligand-residue interaction energies are 1.3, 1.2, and 1.1 times higher than the second highest values, respectively. For 6MITC, 2b, 2c, 2e, and 2h/P-gp, the highest values are much higher than the second highest energies. The highest values for each ITC are enclosed in red rectangles. (B) Graphical presentation of the data in (A). Based on the highest values for the ITC/P-gp ligand-residue interaction energies, the intracellular accumulation of the ITCs (inhibition of P-gp by the ITCs) can be predicted in the order of 6MITC > 2b > 2e > 2c ≈ 2d ≈ 2h ≈ 2f ≈ 2g

Analysis of the interaction energies between the tested ITCs and P-gp

We also analyzed the residues exhibiting the highest interaction energy values for each ITC/P-gp complex to identify the most influential residues for the ITC/P-gp interactions. The ligand-residue interaction energies were calculated by the method of Labute [44], which assigns energy terms in kcal/mol for each residue. Generally, a negative value indicated that the residue attracted the ligand, while a positive value indicated that the residue repelled the ligand. The 3D structures of the LBS and the highest energy values for each ITC/P-gp complex are shown in Figure 3A–H. 6MITC/Gln-725 had the highest interaction energy value of −8.7928 (kcal/mol; Figure 3A), −7.8815 for 2b/Asn-721 (Figure 3B), −2.9168 for 2c/Met-986 (Figure 3C), −2.6632 for 2d/Gln-990 (Figure 3D), −4.8427 for 2e/Asn-721 (Figure 3E), −2.2855 for 2f/Phe-770 (Figure 3F), −2.1786 for 2g/Met-986 (Figure 3G), and −2.4232 for 2h/Asn-721 (Figure 3H). These findings confirmed the importance of residues Asn-721 and Gln-725 for the ITC/P-gp interactions, based on the comparatively high interaction energies of −8.7928 (kcal/mol; 6MITC/Gln-725; Figure 3A), −7.8815 (2b/Asn-721; Figure 3B), and −4.8427 (2e/Asn-721; Figure 3E). No compounds can exert effects without entering the inside of cells, unless their functions are mediated by receptors on the cell membranes. We surmised that the intracellular accumulation of ITCs could be attributed to the binding of the ITCs to P-gp, and therefore conducted further *in silico* structural analyses of the ITC/P-gp model to predict the possible intracellular accumulation of the ITCs. All of the ligand-residue interaction energies for the 12 preferred residues were calculated (Figure 4A), and the values are shown graphically (Figure 4B). The highest values for the 2d, 2f, and 2g/P-gp ligand-residue interaction energies were 1.3, 1.2, and 1.1 times higher than the second highest values, respectively. For 6MITC, 2b, 2c, 2e, and 2h/P-gp, the highest values were much higher than the second highest energies, suggesting that the highest value for the interaction energy is crucial for the ITC/P-gp interactions. With due consideration of these results, we can predict the intracellular accumulation of the ITCs (inhibition of P-gp by the ITCs) in the order of 6MITC > 2b > 2e > 2c ≈ 2d ≈ 2h ≈ 2f ≈ 2g. This order is proposed mostly on the basis of the highest values for the ITC/P-gp interaction energies.

CONCLUSION

In the present study, we performed *in silico* analyses of the ligand-residue interaction between P-gp and 6MITC and its analogs to predict possible inhibitory effects of the ITCs on P-gp. Our results revealed that the tested ITCs could bind to the LBS in P-gp and can predict their biological potency, such as the ability to inhibit P-gp and to accumulate in cells. The ITCs with higher *in silico* ligand-residue interaction energies, that indicate possible higher inhibitory effects on P-gp, may be accumulated at higher concentrations in cells. This suggests that the ITCs showing stronger binding to P-gp possibly function against the P-gp-mediated efflux. To the best of our knowledge, this is the first report to

predict the possible biological potency of ITCs with *in silico* structural analyses between the ITCs and P-gp. *In silico* structural analyses have gained great importance in drug discovery and development [45], and further *in silico* analyses between cancer-related proteins and the ITCs are ongoing in our laboratories to elucidate the more detailed mechanism underlying the inhibitory effects of the ITCs on cancer.

Acknowledgements

This study was partly supported by a Grant-in-Aid from the Promotion and Mutual Aid Corporation for Private Schools of Japan.

REFERENCES

1. Kjaer A (1960). Naturally derived isothiocyanates (mustard oils) and their parent glucosides. Fortschr Chem Org Naturst. 18: 122-176
2. Fenwick GR, Heaney RK and Mullin WJ (1983). Glucosinolates and their breakdown products in food and food plants. CRC Crit Rev Food Sci Nutr. 18: 123-201
3. Shapiro TA, Fahey JW, Wade KL, et al (2001). Chemoprotective glucosinolates and isothiocyanates of broccoli sprouts: metabolism and excretion in humans. Cancer Epidemiol Biomarkers Prev. 10: 501-508
4. Getahun SM and Chung FL (1999). Conversion of glucosinolates to isothiocyanates in humans after ingestion of cooked watercress. Cancer Epidemiol Biomarkers Prev. 8: 447-451
5. Milford GFJ and Evans EF (1991). Factors causing variation in glucosinolales in oil seed rape. Outlook Agrie. 20: 31-37
6. Mullin WJ and Sahasrabudhe HR (1978). An estimate of the average daily intake of glucosinolates. Nutr Rep Int. 18: 273-279
7. Fimognari C and Hrelia P (2007). Sulforaphane as a promising molecule for fighting cancer. Mutat Res. 635: 90-104
8. Zhang Y and Talalay P (1994). Anticarcinogenic activities of organic isothiocyanates: chemistry and mechanisms. Cancer Res. 54: 1976s-1981s
9. Fuke Y, Haga Y, Ono H, et al (1997). Anti-carcinogenic activity of 6-methylsulfinylhexyl isothiocyanate, an active anti-proliferative principal of wasabi (Eutrema wasabi Maxim.). Cytotechnology. 25: 197-203
10. Fimognari C, Nusse M, Cesari R, et al (2002). Growth inhibition, cell-cycle arrest and apoptosis in human T-cell leukemia by the isothiocyanate sulforaphane. Carcinogenesis. 23: 581-586
11. Parnaud G, Li P, Cassar G, et al (2004). Mechanism of sulforaphane-induced cell cycle arrest and apoptosis in human colon cancer cells. Nutr Cancer. 48: 198-206
12. Jackson SJ and Singletary KW (2004). Sulforaphane inhibits human MCF-7 mammary cancer cell mitotic progression and tubulin polymerization. J Nutr. 134: 2229-2236
13. Singh AV, Xiao D, Lew KL, et al (2004). Sulforaphane induces caspase-mediated apoptosis in cultured PC-3 human prostate cancer cells and retards growth of PC-3 xenografts in vivo. Carcinogenesis. 25: 83-90
14. Myzak MC, Dashwood WM, Orner GA, et al (2006). Sulforaphane inhibits histone deacetylase in vivo and suppresses tumorigenesis in Apc-minus mice. FASEB J. 20: 506-508
15. Guo Z, Smith TJ, Wang E, et al (1992). Effects of phenethyl isothiocyanate, a carcinogenesis inhibitor, on xenobiotic-metabolizing enzymes and nitrosamine metabolism in rats. Carcinogenesis. 13: 2205-2210
16. Gamet-Payrastre L, Li P, Lumeau S, et al (2000). Sulforaphane, a naturally occurring isothiocyanate, induces cell cycle arrest and apoptosis in HT29 human colon cancer cells. Cancer Res. 60: 1426-1433
17. Pham NA, Jacobberger JW, Schimmer AD, et al (2004). The dietary isothiocyanate sulforaphane targets pathways of apoptosis, cell cycle arrest, and oxidative stress in human pancreatic cancer cells and inhibits tumor growth in severe combined immunodeficient mice. Mol Cancer Ther. 3: 1239-1248
18. Singh SV, Herman-Antosiewicz A, Singh AV, et al (2004). Sulforaphane-induced G2/M phase cell cycle arrest involves checkpoint kinase 2-mediated phosphorylation of cell division cycle 25C. J Biol Chem. 279: 25813-25822
19. Traka M, Gasper AV, Smith JA, et al (2005). Transcriptome analysis of human colon Caco-2 cells exposed to sulforaphane. J Nutr. 135: 1865-1872
20. Hong F, Freeman ML and Liebler DC (2005). Identification of sensor cysteines in human Keap1 modified by the cancer chemopreventive agent sulforaphane. Chem Res Toxicol. 18: 1917-1926
21. Prestera T, Holtzclaw WD, Zhang Y, et al (1993). Chemical and molecular regulation of enzymes that detoxify carcinogens. Proc Natl Acad Sci USA. 90: 2965-2969
22. Smith TJ, Hong JY, Wang ZY, et al (1995). How can carcinogenesis be inhibited? Ann NY Acad Sci. 768: 82-90
23. Primiano T, Sutler TR and Kensler TW (1997). Antioxidant-inducible genes. Advan Pharmacol. 38: 293-328
24. Hecht SS (1997). Approaches to cancer prevention based on an understanding of N-nitrosamine carcinogenesis. Proc Soc Exp Biol Med. 216: 181-191
25. Kensler TW (1997). Chemoprevention by inducers of carcinogen detoxification enzymes. Environ Health Perspect. 105 (Suppl.): 964-970
26. Traka MH, Spinks CA, Doleman JF, et al (2010). The dietary isothiocyanate sulforaphane modulates gene expression and alternative gene splicing in a PTEN null preclinical murine model of prostate cancer. Mol Cancer. 9: 189
27. Schinkel AH and Jonker JW (2003). Mammalian drug efflux transporters of the ATP binding cassette (ABC) family: an overview. Adv Drug Deliv Rev. 55: 3-29
28. Pastan I and Gottesman MM (1991). Multidrug resistance. Annu Rev Med. 42: 277-286
29. Bradshaw DM and Arceci RJ (1998). Clinical relevance of transmembrane drug efflux as a mechanism of multidrug resistance. J Clin Oncol. 16: 3674-3690
30. Hu K and Morris ME (2004). Effects of benzyl-, phenethyl-, and alpha-naphthyl isothiocyanates on P-glycoprotein- and MRP1-mediated transport. J Pharm Sci. 93: 1901-1911
31. Noshita T, Kidachi Y, Funayama S, et al (2009). Anti-nitric oxide production activity of isothiocyanates correlates with their polar surface area rather than their lipophilicity. Eur J Med Chem. 44: 4931-4936
32. Nomura T, Shinoda S, Yamori T, et al (2005). Selective sensitivity to wasabi-derived 6-(methylsulfinyl)hexyl isothiocyanate of human breast cancer and melanoma cell lines studied in vitro. Cancer Detect Prev. 29: 155-160
33. Fuke Y, Shinoda S, Nagata I, et al (2006). Preventive effect of oral administration of 6-(methylsulfinyl)hexyl isothiocyanate derived from wasabi (Wasabia japonica Matsum) against pulmonary metastasis of B16-BL6 mouse melanoma cells. Cancer Detect Prev. 30: 174-179
34. Yamaguchi H, Kidachi Y, Kamiie K, et al (2012). Homology modeling and structural analysis of human P-glycoprotein. Bioinformation. 8: 1066-1074
35. Aller SG, Yu J, Ward A, et al (2009). Structure of P-glycoprotein reveals a molecular basis for poly-specific drug binding. Science. 323: 1718-1722
36. Levitt M (1992). Accurate modeling of protein conformation by automatic segment matching. J Mol Biol. 226: 507-533
37. Fechteler T, Dengler U and Schomberg D (1995). Prediction of protein three-dimensional structures in insertion and deletion regions: a procedure for searching data bases of representative protein fragments using geometric scoring criteria. J Mol Biol. 253: 114-131
38. Goto J, Kataoka R, Muta H, et al (2008). ASEDock-docking based on alpha spheres and excluded volumes. J Chem Inf Model. 48: 583-590
39. Halgren TA (1996). Merck molecular force field. I. Basis, form, scope, parameterization, and performance of MMFF94. J Comput Chem. 17: 490-519
40. Tseng E, Kamath A and Morris ME (2002). Effect of organic isothiocyanates on the P-glycoprotein- and MRP1-mediated transport of daunomycin and vinblastine. Pharm Res. 19: 1509-1515

41. Wise JG (2012). Catalytic transitions in the human MDR1 P-glycoprotein drug binding sites. Biochemistry. 51: 5125-5141
42. Goto J, Kataoka R, Muta H, et al (2008). ASEDock-docking based on alpha spheres and excluded volumes. J Chem Inf Model. 48: 583-590
43. Kolm RH, Danielson UH, Zhang Y, et al (1995). Isothiocyanates as substrates for human glutathione transferases: structure-activity studies. Biochem J. 311: 453-459
44. Labute P (2008). The generalized Born/volume integral implicit solvent model: estimation of the free energy of hydration using London dispersion instead of atomic surface area. J Comput Chem. 29: 1693-1698
45. Jorgensen WL (2004). The many roles of computation in drug discovery. Science. 303: 1813-1818

*****